Improving direct normal irradiance retrieval in cloud-free, but high aerosol load conditions by using aerosol optical depth

M. Boraiy, M. Korany, Y. Aoun, S.C. C Alfaro, M. El-Metwally, M M Abdel Wahab, Philippe Blanc, Y. Eissa, H. Ghedira, G. Siour, et al.

Meteorologische Zeitschrift, Vol. **26**, No. 5, 475–483 (published online September 24, 2017)

Improving direct normal irradiance retrieval in cloud-free, but high aerosol load conditions by using aerosol optical depth

M. Boraiy[1], M. Korany[2], Y. Aoun[3], S.C. Alfaro[4*], M. El-Metwally[5], M.M. Abdel Wahab[6], P. Blanc[3], Y. Eissa[7], H. Ghedira[7], G. Siour[4], K. Hungershoefer[8] and L. Wald[3]

[1]Physics and Mathematical Engineering Department, Faculty of Engineering, Port Said University, Port Said, Egypt
[2]Egyptian Meteorological Authority, Cairo, Egypt
[3]MINES ParisTech, PSL Research University, O.I.E. – Centre Observation, Impacts, Energy, Sophia Antipolis, France
[4]Laboratoire Inter-universitaire des Systèmes Atmosphériques, Universités de Paris-Est Créteil et Paris-Diderot, Créteil, France
[5]Physics Department, Faculty of Science, Port Said University, Port Said, Egypt
[6]Astronomy and Meteorology Department, Faculty of Science, Cairo University, Cairo, Egypt
[7]Masdar Institute, Research Center for Renewable Energy Mapping and Assessment, Abu Dhabi, UAE
[8]Deutscher Wetterdienst, Offenbach, Germany.

(Manuscript received December 5, 2016; in revised form April 14, 2017; accepted April 26, 2017)

Abstract

Measurements of the global surface solar irradiation and its direct and diffuse components performed at three Egyptian sites (Aswan, Cairo, and Port Said) are used to test the ability of two published decomposition models to estimate the hourly direct normal irradiance from the measured global horizontal one in cloud-free conditions. The tested models failed to reproduce the temporal variability of the measurements, which we show to be partly induced by the large variability of the atmospheric content in aerosols. We propose a revised formulation of the decomposition models that takes into account the aerosol optical depth (AOD) at 1000 nm derived from onsite measurements. It leads to a significant reduction of the bias and root mean square deviation of the original models and this at the three Egyptian sites. However, because the AOD is rarely measured at the meteorological stations, we also quantify the performance of the revised models when the AOD is either derived from the MODIS observations or obtained by the products from Copernicus Atmospheric Monitoring Service (CAMS). Probably because of their finer temporal resolution that makes them more apt to reproduce the rapid variations of the AOD, the best results are obtained with the CAMS products. Therefore, we recommend using a combination of the revised decomposition models and these CAMS products to estimate the hourly direct normal irradiance in areas such as Egypt where aerosols are ubiquitous. Note that the improved decomposition models are generally applicable in all-sky conditions, although their benefit has been demonstrated to be significant, and probably limited to, cloud-free conditions.

Keywords: Direct normal irradiance, Aerosols, Egypt, MENA

1 Introduction

The countries of the Middle East and North Africa region (MENA) are currently working on partly meeting their electricity demands from solar powered plants (Griffiths, 2013; Brand and Zingerle, 2011; Bryden et al., 2013). For instance, Egypt is planning to increase rapidly the share of solar energy in its electricity production and to have installed by year 2017 a capacity of 2.3 GW of solar powered plants (El Sobki, 2015). This goal can only be achieved by increasing the number of classical photovoltaic (PV) systems and by implementing new large scale concentrated solar power (CSP) units. Contrary to PV technology, that exploits the global irradiance (G) reaching the Earth's surface, CSP converters are sensitive only to its direct component received at normal incidence, the so-called direct normal irradiance DNI (B_n). Therefore, the evaluation of the potential of these future CSP production units requires an accurate assessment of this direct component.

Pyrheliometers are instruments for measuring B_n. They are very rare because they are expensive and costly to maintain for long periods because they must be mounted on a sun-tracking device. Measurements of G are more frequent and many models have been published to estimate B_n from the sole knowledge of G. These models are very often empirical and are called decomposition models because they split G into its diffuse D and B components on a horizontal surface. Then, B_n is computed by dividing B by $cos(Z)$ where Z is the solar zenith angle.

*Corresponding author: Stephane Alfaro, Laboratoire Inter-universitaire des Systèmes Atmosphériques, UMR CNRS 7583, Universités de Paris-Est Créteil et Paris-Diderot, 61 Avenue du Généralde Gaulle, 94010 Créteil, France, e-mail: alfaro@lisa.u-pec.fr.

DOI 10.1127/metz/2017/0844
Gebrüder Borntraeger Science Publishers, Stuttgart, www.borntraeger-cramer.com

Table 1: Locations and types of measurements performed at the three sites considered in this study.

Station	Geographical coordinates	Measurement Period	Climate
PSU	31.27° N; 32.28° E; 21 m	February-October 2015	Mediterranean climate
Cairo	30.08° N; 31.28° E; 35 m	2004–2010	Urban-influenced climate
Aswan	23.97° N; 32.78° E; 192 m	2004–2010	Desert Nile climate

The cores of these decomposition models are empirical equations obtained by fitting mathematical equations to long-term observations of G and D, or G and B_n, made at one or a few sites. These equations relate the diffuse fraction (k_d), defined as D/G – or the direct beam transmittance ($k_b = B_n$/extraterrestrial normal irradiance) – to the clearness index ($k_t = G$/extraterrestrial horizontal irradiance). These decomposition models are very popular. They are also used in satellite-based retrieval of G and its two components. These models are based on original measurements performed most often in North America or in Europe. However, the question of their applicability to other regions of the world is open, especially where the aerosol effect on the DNI is large like in areas such as the Mediterranean basin, which is influenced by desert dust intrusions and intense anthropogenic activities (Nikitidou et al., 2014). This is also the case of the MENA region, including Egypt, where the aerosols are known to be not only highly variable in concentration and types but also to differ notably in composition from those of the western countries (Alfaro and Abdel Wahab 2006; Mahmoud et al., 2008; Favez et al., 2008; El-Metwally et al., 2008, 2011).

The present article proposes to include aerosols in empirical decomposition models to improve their performances. To that aim, two decomposition models have been arbitrarily selected among those published that have been established for the Mediterranean climate. They were tested against measurements of G, D and B_n made at three Egyptian experimental sites (Port Saïd, Cairo, and Aswan) fully equipped for the measurement of the global solar irradiance and its direct and diffuse components. Then, an improvement is proposed to include the aerosol optical depth in the models and the benefit of the improved models is demonstrated. To better evidence the role of aerosols and the benefit of the proposed improvement, the present work is restricted to cloud-free conditions for which the influence of the aerosols is at its highest.

2 Measurements and methods

2.1 Experimental sites

The climate of Egypt is governed mainly by its location in the northeastern part of Africa on the margin of the largest desert in the world. Its latitudinal position, between 22° and 32° N places it in the sub-tropical dry belt, although weather on its northern coast is impacted by the presence of the sea. Generally, climate

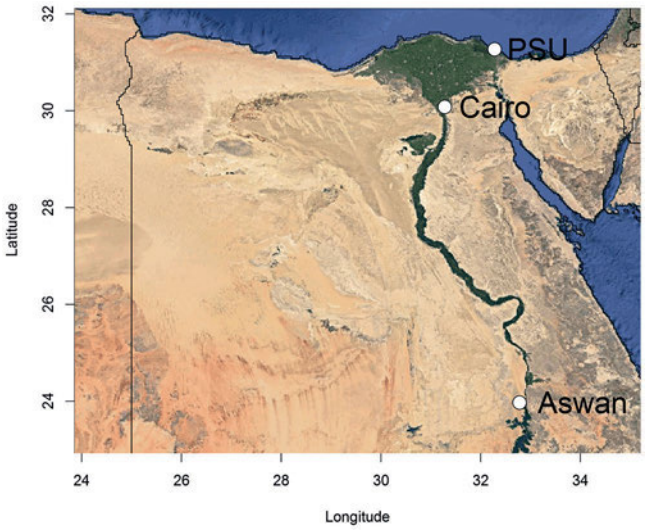

Figure 1: Locations of the three sites selected for this study.

in Egypt can be expressed as a contest between the hot and dry air masses of the Sahara and the cooler, damper maritime air masses from the north. In spring, eastward moving depressions are frequent, and in winter, the air masses coming from the north can bring rain with them in particular along the Egyptian Mediterranean coast. For more details, we refer the reader to El-Wakil et al. (2001) or El-Metwally and Alfaro (2013). In the present study, three sites have been selected along a North-South axis (Fig. 1, Table 1); they represent different types of Egyptian climates (Diabaté et al., 2004). The southernmost one is the Aswan meteorological station of the Egyptian Meteorological Authority (EMA). It has a dry desert climate. The second one, also run by the EMA, is located in Greater Cairo, which is a very large, densely populated and industrialized area characterized by a semi-arid warm dry climate with a boreal summer dry season. The third site is the experimental station of Port Said University (PSU). This site of the Eastern Mediterranean coast is characterized by a rainy climate with mild winters.

2.2 Irradiance measurements and data quality control

The three selected stations are equipped with pyranometers measuring G and D and pyrheliometers measuring B_n. Table 1 summarizes the characteristics (location, type of climate) of the experimental sites and the periods of measurements.

At the EMA stations, instruments are Eppley precision spectral pyranometers (PSP) and Normal Incidence Pyrheliometers (NIP). These instruments are calibrated each year against a reference instrument that participate in the International Pyrheliometric Comparisons (IPC) every five years and is traceable to the World Radiometric Reference (WRR) maintained at Davos, Switzerland (WRC, 1985, 1995). According to the final report of the twelfth WMO International Pyrheliometer Comparison (WMO-IMO, 2016) held from 28 September to 16 October 2015 in Davos, Switzerland, the stated uncertainty of the WRR is 0.4 %. The achievable uncertainty of calibration is < 2 % for the two instruments, whereas for the measurements performed with the PSP and NIP it is approximately 3–5 and 1–2 %, respectively (El-Metwally, 2004; Omran, 2000; El-Wakil et al., 2001). The datasets of the EMA have been extensively described in Korany et al. (2016) and are freely available online at https://doi.pangaea.de/10.1594/PANGAEA.848804.

At PSU, a pyrheliometer (EKO, model MS56) mounted on a sun tracker (EKO, model 22G) was used to measure B_n, a shaded pyranometer (EKO, model MS802) to measure the diffuse component (D), and a pyranometer (LSI LASTEM, model DPA 153) to measure G. According to their certificates of calibration, the sensitivities of these instruments are $7.711 \pm 0.063 \mu v/W/m^2$ (± 0.5 %), $7.12 \pm 0.012 \mu v/W/m^2$ (0.63 %) and $50.5 \pm 2.36 \mu v/W/m^2$ (± 4.7 %) respectively.

At the three sites, data-loggers scan the signals from the radiation sensors at least every minute. However, these initial data are stored as hourly averages in the data-logger (Korany et al., 2016).

Only cases corresponding to solar zenith angles less than 85° have been retained in this study to avoid cosine response problems of the radiometric sensors. The quality of the radiometric observations has also been controlled carefully following the procedure described in Korany et al. (2016). Briefly, the quality check involves a series of tests aiming at determining whether the measurements lie within expected boundaries and limits and are therefore acceptable, or not. These tests are guided either by physical reasoning (to detect physically impossible events) or by the statistical variability of the data (to detect very rare and thus questionable events). Furthermore, they treat the global and its two components separately, and then compare them to each other. In addition, because the lowest values can be noise only and may have no significance, B_n must be greater than $5\ W\ m^{-2}$, which is approximately 1.5 times the requirement set by WMO/CIMO (2014) for measurements of hourly mean of direct normal irradiance of good quality. By rejecting B_n less than $5\ W\ m^{-2}$, there is 0.3 % chance of having insignificant very low values.

Finally, cloud-contaminated situations have been discarded by applying the following restrictions: 1) Only data collected at times when direct observations of the sky were performed by human observers have been considered, 2) cloudiness at the times of these measurements should not exceed 2 oktas, and 3) only conditions of clear line of sight (i.e., no clouds in front of, or close to, the solar disk) have been retained.

2.3 Quantification of the atmospheric content in aerosols

There are several options to quantify the amount of aerosols in the atmosphere and their direct impact on radiative transfer. The most accurate way consists in measuring their optical depth (AOD) at discrete wavelengths of the solar spectrum with a spectral sunphotometer such as those of the AErosol RObotics NETwork (http://aeronet.gsfc.nasa.gov/) (Holben et al., 1998). Such a spectral sunphotometer is installed at Cairo. Measurements are not made as regularly as measurements of G, D and B_n, and there are few coincident measurements.

When no sunphotometer measurement is available, the AOD must be obtained by indirect methods. The first possibility consists in using the method of Gueymard (1998) to estimate the AOD at 1000 nm from the measurements of B_n. This AOD at 1000 nm is also called the Angström turbidity coefficient and is noted β in the following.

When neither the sunphotometric or pyrheliometric measurements necessary for the estimation of the AOD are performed onsite, the observations of satellite-borne spectrometers such as Moderate Resolution Imaging Spectroradiometers (MODIS) aboard Aqua and Terra can be inverted to retrieve an estimate of the AOD at specific wavelengths (Gupta et al., 2013; Jalal et al., 2015; El-Metwally et al., 2010). In this study, when they are available we will use the two values per day of the AOD at 550 nm (AOD_{550}) retrieved by MODIS in the pixels containing the three Egyptian stations. Alternatively, the atmospheric models developed to simulate emission, transport and deposition of the main components (sea-salt, mineral dust, sulfates, black carbon, and organic carbon) of the atmospheric aerosol can be used. Indeed, the numerous outputs of these models usually include the AOD at different solar wavelengths. In this work, we use the products of the Copernicus Atmospheric Monitoring Service (CAMS: https://atmosphere.copernicus.eu/), which consolidates many years of preparatory research and development funded by the European Union in the form of the series of MACC (http://macc.copernicus-atmosphere.eu/) projects. Of particular interest for this study, the total AOD at 550 nm (AOD_{550}) is computed every 3 h with a spatial resolution of 0.75° (Morcrette et al., 2009). These AOD_{550} are interpolated spatially and temporally to make them coincide with the hourly measurements performed at the three Egyptian stations.

2.4 The decomposition models to estimate B_n from G

A large number of decomposition models have been published to estimate B_n when only G is measured or

available from satellite-based retrievals It is not the objective of this work to make an exhaustive review of the performances of the existing models (for such a review, on can refer to Gueymard and Ruiz-Arias, 2016). We rather aim to show how they can be improved in areas such as Egypt where aerosols play a major role on the atmospheric transfer of solar radiation. Therefore, we have arbitrarily selected two published and well-used decomposition models that have been set for the Mediterranean climate: Model1 is that of Louche et al. (1991), and Model2 that of López et al. (2000).

Model 1

Based on G and B_n data measured at Ajaccio (Corsica, France, 44.9° N) between October 1983 and June 1985, Louche et al. (1991) proposed a model expressing B_n as a function of the irradiance at the top of atmosphere at normal incidence (B_{n0}) and $k_t$only:

$$B_n = B_{n0}\,(-10.627k_t^5 + 15.307k_t^4 - 5.205k_t^3 + 0.994k_t^2 - 0.059k_t + 0.002) \quad (2.1)$$

Model 2

López et al. (2000) used the measurements performed at six different Spanish stations to propose a polynomial empirical parameterization of the correlation linking k_b to k_t. After this initial adjustment, they attributed the residual dispersion of the observed values of k_b for a given k_t to the variability of Z. The corresponding equations are the following:

$$\begin{aligned} k_b &= k_t^2(0.928 - 0.909\cos Z) && k_t \le 0.325 \\ k_b &= 0.069 - 0.475k_t + 1.733k_t^2 - 0.096\cos Z && k_t \ge 0.325 \end{aligned} \quad (2.2)$$

2.5 Quantification of the performance of models

Statistical quantities such as the bias, root mean square deviation (RMSD), and coefficient of determination (R^2) are used for comparing the outputs of the models to the reference observations and thus quantifying theirs individual performances:

$$\begin{aligned} Bias &= \frac{1}{n}\sum_{i=1}^{n}(e_i) \\ RMSD &= \sqrt{\frac{1}{n}\sum_{i=1}^{n}(e_i)^2} \end{aligned} \quad (2.3)$$

where $e_i = P_i - M_i$ is the difference between the predicted (P_i) and the observed (M_i) values. Relative values of the bias and RMSD are obtained by dividing them by the mean ($\overline{M}$) of the observations.

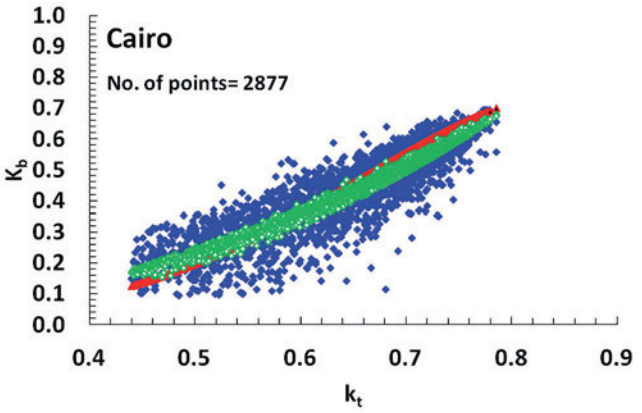

Figure 2: Variation with k_t of k_b observed (blue points) and simulated by Model1 (red points) and Model2 (green points) at the Cairo experimental station.

Table 2: Statistical indicators of the performance of the two decomposition models used for estimating B_n (in W m^{-2}) at the three Egyptian sites.

Site	No. of samples	Mean Value	Indicators	Model1	Model2
PSU	1350	729	*rBias*	−0.02	−0.08
			rRMSD	0.11	0.15
			R^2	0.78	0.71
Cairo	2877	598	*rBias*	0.04	−0.01
			rRMSD	0.16	0.13
			R^2	0.78	0.80
Aswan	3611	726	*rBias*	0.02	−0.03
			rRMSD	0.13	0.13
			R^2	0.73	0.72

3 Performance of the two models

In order to check the ability of the decomposition models to derive correctly k_b from k_t, their predictions can be compared to the observations. The examination of the results for Cairo (Fig. 2) reveals that the general trend is correct but that the decomposition models fail to reproduce the dispersion of the experimental values of k_b observed in any given range of k_t.

Quantitatively, this is reflected by the relatively low values of the *rBias* (4 and −1 %) but significantly larger one of the *rRMSD* (16 and 13 %) of Model1 and Model2, respectively, when they are used to estimate B_n (Table 2). Similar results are obtained at the other two sites (Table 2).

In order to check if the variability of the aerosol loading of the atmosphere is responsible for the incapacity of the models to simulate k_b correctly, we plotted the relative error $(k_{b,\text{model}} - k_{b,\text{observed}})/k_{b,\text{observed}}$ as a function of a proxy of the aerosol loading. At the three stations, β deduced from hourly pyrheliometer measurements is such a proxy. We added AOD_{440} measured at the Cairo AERONET station. Fig. 3 displays the relative errors of Model1 and Model2 plotted as a function of β and

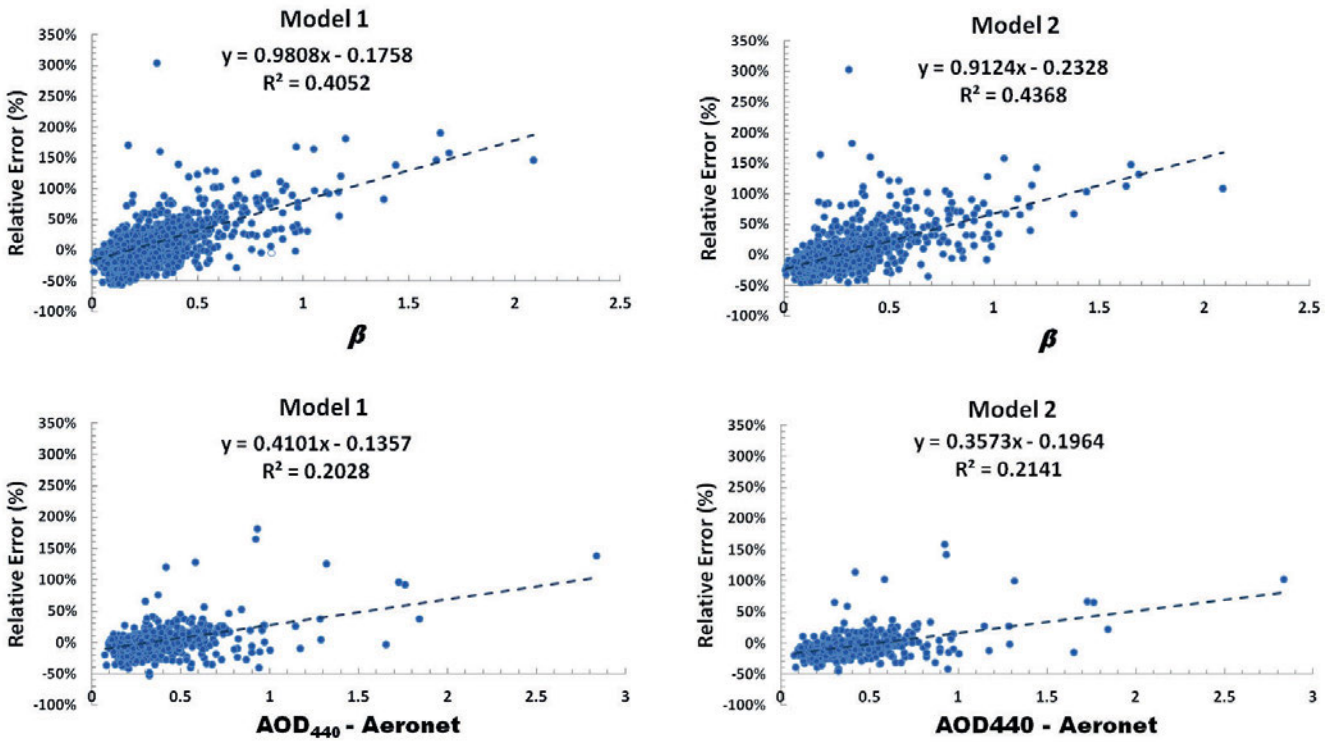

Figure 3: Relative error of the two tested decomposition models as a function of β computed from the pyrheliometer measurements (upper row) and AOD_{440} from the AERONET station (lower row). There are fewer sunphotometer (543) measurements than pyrheliometer (2877) ones in the period of study at Cairo.

AOD_{440} at Cairo. In spite of a relatively large scatter denoted by low values of R^2, the relative errors obviously tends to increase with either β or AOD_{440}. Similar results (not shown) are obtained with β for the sites of Aswan and Port Said. This shows that if the current decomposition models fail to reproduce the dispersion of the k_b measurements in Egypt, this is at least in part because they do not account for the large variability of the atmospheric content in aerosols.

4 Pyrheliometer-based correction of the decomposition models

A simple approach is devised to include the aerosols in the decomposition models, whose relative errors are assumed to increase linearly with β:

$$(k_{b,\text{model}} - k_{b,\text{observed}})/k_{b,\text{observed}} = a\beta + b \qquad (4.1)$$

For the two models, the parameters a and b are obtained by least-square fitting and reported in Table 3, together with R^2. For each model, a and b are similar for the three sites, an observation consistent with the well-known fact that the main variable controlling the impact of the aerosols on B_n is their optical depth rather than their nature, which is most probably different at the marine, urban and desert sites.

Table 3: Slope (a), intercept (b) and coefficient of determination (R^2).

	Model1			Model2		
	PSU	Cairo	Aswan	PSU	Cairo	Aswan
a	1.15	0.98	1.29	1.06	0.91	1.24
b	−0.14	−0.17	−0.16	−0.17	−0.23	−0.19
R^2	0.53	0.41	0.48	0.38	0.44	0.47

Equation (4.1) shows that it is possible to modify the original decomposition models to make them predict k_b values more in agreement with the observations:

$$k_{b,\text{new model}} = k_{b,\text{model}}/(a\beta + b + 1) \qquad (4.2)$$

Combining this equation with equations (2.1) and (2.2), one finally obtains a revised version of Model1 and Model2 based on the pyrheliometer measurements, hereinafter referred to as Model1B_Pyr and Model2B_Pyr respectively:

$$k_{b,\text{model1B}} = (-10.627k_t^5 + 15.307k_t^4 - 5.205k_t^3 + 0.994k_t^2 - 0.059k_t + 0.002)/(a\beta + b + 1) \qquad (4.3)$$

$$k_{b,\text{model2B}} = (0.069 - 0.475k_t + 1.733k_t^2 - 0.096\cos Z)/(a\beta + b + 1) \qquad k_t \geq 0.325 \qquad (4.4)$$

When comparing the values of k_b predicted by the two new models for Cairo with the measured values

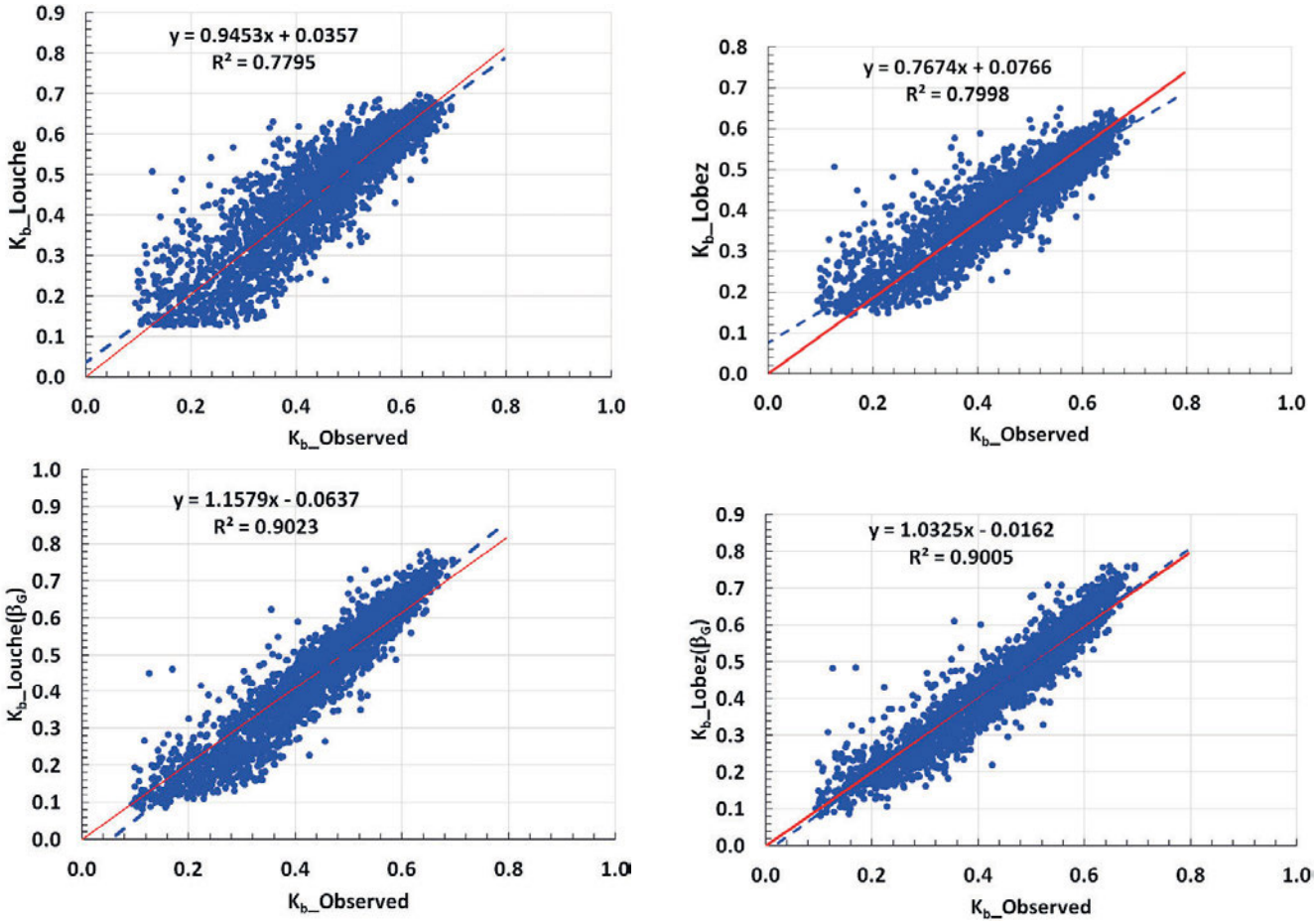

Figure 4: Comparison with the reference measurements of the k_b values yielded by the un-corrected models (top row) and by their corrected versions Model1B_Pyr (left panel, bottom row) and Model2B_Pyr (right panel, bottom row). The case presented is the one of Cairo.

Table 4a: Results of the comparison of B_n predicted by the original Model1 and by the new Model1B_Pyr. *Bias* and *RMSD* are in W m^{-2}.

	PSU		Cairo		Aswan	
	Model1	Model1B_Pyr	Model1	Model1B_Pyr	Model1	Model1B_Pyr
Bias	−17.87	−0.83	24.61	13.91	17.48	8.69
rBias	−0.02	0.001	0.04	0.02	0.02	0.01
RMSD	80.90	57.33	93.65	74.23	96.11	72.09
rRMSD	0.11	0.08	0.16	0.12	0.13	0.10
R^2	0.78	0.89	0.78	0.91	0.73	0.89

Table 4b: Results of the comparison of B_n predicted by the original Model2 and by the new Model2B_Pyr. *Bias* and *RMSD* are in W m^{-2}.

	PSU		Cairo		Aswan	
	Model2	Model2B_Pyr	Model2	Model2B_Pyr	Model2	Model2B_Pyr
Bias	−57.65	−15.77	−5.54	−2.55	−18.21	0.28
rBias	−0.08	−0.02	−0.01	−0.004	−0.03	0.0004
RMSD	110.07	78.50	80.14	61.20	91.97	76.16
rRMSD	0.15	0.11	0.13	0.10	0.13	0.10
R^2	0.71	0.79	0.80	0.90	0.72	0.85

(Fig. 4) a much better agreement is obtained than with Model1 and Model2. Indeed, the statistical indicators (Table 4a, 4b) show that generally Model1B_Pyr and Model2B_Pyr perform better than their original versions and this at the three Egyptian sites of this study. More precisely, with the inclusion of the information on the AOD the bias of Model2 is reduced from −58 to −16 W m^{-2} at PSU and becomes negligible (< 3 W m^{-2})

Table 5: Slope (a), intercept (b), and coefficient of determination (R^2) obtained for Model2 modified to input AOD from three different sources (MODIS, CAMS, and Pyrheliometer).

	MODIS			CAMS			Pyrheliometer		
	PSU	Cairo	Aswan	PSU	Cairo	Aswan	PSU	Cairo	Aswan
a	0.34	0.36	0.41	0.38	0.46	0.47	1.06	0.91	1.24
b	−0.15	−0.07	−0.14	−0.15	−0.11	−0.16	−0.17	−0.23	−0.19
R^2	0.17	0.05	0.11	0.19	0.07	0.12	0.38	0.44	0.47

at Aswan and Cairo. For this model, the RMSD decreases by as much as 32, 19 and 15 W m^{-2} at PSU, Cairo and Aswan, respectively. Similarly good results are obtained with Model1B. This shows that the two revised models are much more able to capture the dispersion of the measurements than the uncorrected ones. Model1B_Pyr performs slightly better in PSU and Aswan than Model2B_Pyr and conversely in Cairo but overall the performances of the two revised models are quite comparable.

5 Using the CAMS and MODIS AOD to correct the decomposition models

We have shown that because they do not account for the variability of the atmospheric content in air-suspended particles, the performances of the decomposition models are not as good in Egypt, and probably beyond in the whole MENA region, as they are in western countries. In addition, we have shown that it was possible to improve the performances of the original models by incorporating into their equations a correction, which is a function of the content of aerosols integrated along the vertical in the atmosphere. So far, in our calculations we have chosen the aerosol optical depth at 1000 nm (β) as a proxy of this columnar content. This was possible only because the pyrheliometer measurements necessary for the calculation of β were performed at the three Egyptian sites considered in this study. Unfortunately, at most meteorological stations these measurements are not available and this is why we need to estimate B_n by indirect methods in the first place. The sites where the AOD is measured directly with a spectral sunphotometer are even fewer in North Africa and the Middle East. As substitutes to these lacking measurements, one can use either the AOD obtained by inversion of the observations of satellite-borne sensors or the AOD predicted by models simulating the emission, transport, and deposition of the aerosols. The main advantage of these two types of alternate methods is their global spatial coverage. Among their possible drawbacks, one can cite the fact that the AOD is not the product of a direct measurement. In addition, their spatial and temporal resolutions are not as fine as are those of the sunphotometer and pyrheliometer measurements and an interpolation is necessary. The resulting uncertainties on the determination of the AOD probably lead to a degradation of the benefit of the improvement we have proposed for the decomposition models. In order to quantify precisely the magnitude of this degradation, we have selected arbitrarily Model2 to apply our method but with a correction based either on the AOD derived from the observations of MODIS or on the AOD provided by CAMS products and interpolated both spatially and temporally to coincide with the measurements performed at the three experimental sites. The corresponding upgraded versions of Model2 will be referred to as Model2B_MOD and Model2B_CAMS, respectively. The results of the linear adjustment of the relative error of Model2 on the determination of k_b are reported in Table 5. Note that to facilitate the comparison with the previous adjustment as a function of β, the results of Table 3 for Model2 have also been included in this Table.

Table 6: Comparison of the performances of Model2B_MOD and Model2B_CAMS with those of Model2B_Pyr and the uncorrected Model2 in the retrieval of B_n. *Bias* and *RMSD* are in W m^{-2}.

	Model	Bias	rBias	RMSD	rRMSD	R^2
PSU	2 original	−57.7	−0.08	110.1	0.15	0.71
	2B_Pyr	−15.8	−0.02	78.5	0.11	0.79
	2B_MOD	−12.4	−0.02	91	0.12	0.72
	2B_CAMS	−12.6	−0.02	87.9	0.12	0.72
Cairo	2 original	−5.7	−0.01	80.1	0.13	0.8
	2B_Pyr	−3	0	60.9	0.1	0.9
	2B_MOD	20	0.03	90.8	0.15	0.77
	2B_CAMS	−17	−0.03	78.8	0.13	0.81
Aswan	2 original	−18.2	−0.03	92	0.13	0.72
	2B_Pyr	0.3	0	76.2	0.1	0.85
	2B_MOD	−12.2	−0.02	86.9	0.12	0.74
	2B_CAMS	−13.4	−0.02	84.7	0.12	0.75

As expected, the coefficient of determination for the MODIS or CAMS case is not as strong as for the pyrheliometer case. In spite of this, using the parameters (a, b) of the linear fits to correct Model2 improves the retrieval of k_b, and therefore of B_n at PSU and Aswan (Table 6). The bias of Model2 at PSU decreases from −57.7 to −12.6 W m^{-2} and the RMSD from 110 to 90 W m^{-2} when using the MODIS or CAMS-based corrections. Improvement is also observed at Aswan though less spectacular. As compared to those of Model2, the bias is reduced by 5 to 6 W m^{-2} and the RMSD by 5 to 7 W m^{-2} with Model2B_MOD and Model2B_CAMS. The case of Cairo is more complex. At this site, using the MODIS correction does not reduce the bias or

the RMSD. On the contrary, there is a slight increase in bias and in RMSD. With Model2B_CAMS the bias and RMSD compare to those of Model2. Finally, it appears that using Model2B_CAMS is the best option for retrieving B_n from the G measurements performed at any of the three Egyptian sites if one assumes that β cannot be derived from pyrheliometer measurements. If this choice does not constitute a substantial improvement over Model2 at the urban site of Cairo, it definitely does at both the marine and desert sites. Though this has not been shown in this study, it is highly probable that the poor performance of Model2_MOD in Cairo could be explained by the difficulty of a daily, single-pass, satellite observation to represent correctly the rapid variations of the AOD of the complex particulate mixtures found in this area (El Metwally et al., 2008, 2011). Conversely, with its finer 3-h resolution the CAMS products seems to be more apt to simulate these temporal variations, and particularly at the two sites of Port Said and Aswan where the aerosol situation is assumedly less complex than in Cairo. Though not reproduced here, the results obtained with Model 1 confirm the benefit of using Model1_CAMS or, though to a lesser extent Model1_MOD, rather than the original un-corrected model.

6 Conclusion

In this study, we have shown that the decomposition models available in the literature for deriving the direct normal irradiance from the measured horizontal one fail to reproduce the dispersion of the measurements performed in cloud-free conditions in Egypt. This is also a direct result of the fact that these decomposition models do not integrate any specific information on the content of the atmosphere in aerosols, which is highly variable in this country and more generally in the countries of the Middle East and North Africa. It has been demonstrated that a fairly simple inclusion of the AOD in the two selected models of Louche et al. (1991) and López et al. (2000) improves the performance of these models. Though not done here, it is likely that the improvement would be as easy to include in models other than the two ones selected for this study.

Obviously, the influence of the aerosols is at its highest in cloud-free conditions but decreases strongly with the increasing role of clouds. Oumbe et al. (2014) have shown that in all-sky conditions the global and direct irradiances may be approximated to a high degree of accuracy by tuning down the irradiance of cloud-free conditions by a factor depending mostly on the solar zenith angle, cloud properties and ground albedo. This general method applies to all the models, including those of the above study for which the proposed modification applies initially only to the cloud-free part. It follows that the improved models are expected to be generally applicable in all-sky conditions, although their benefit has been demonstrated to be significant, and probably limited to, cloud-free conditions.

The improvements of the performances of the models depend on how the AOD has been determined. These performances are the best when the AOD is measured directly onsite, but because this is rarely the case, two alternative methods for the determination of the AOD have also been tested: 1) the inversion of the measurements of a satellite-borne spectrometer (MODIS), and 2) the output of the CAMS aerosol models. Probably because its finer temporal resolution allows him to simulate more precisely the rapid variations of the AOD, CAMS is found to provide better results than MODIS. Another advantage of CAMS is that it can be used in a predictive mode, which makes it a suitable tool for nowcasting applications.

Acknowledgments:

This work is a contribution to the SUSIE (SUrface Solar Irradiance in Egypt for energy production) project (#5404) co-funded by the Science and Technology Development Fund (STDF) of Egypt and the French AIRD and of the MISRA project funded by the French Ministry of Foreign Affairs (convention n° EJ 2101638786) and the UAE government. The authors thank the Egyptian Meteorological Authority (EMA) for generously providing the solar radiation and meteorological measurements. The authors are thankful to the AERONET teams for their effort in establishing and maintaining the AERONET network, and to the European Copernicus Programme for establishing and maintaining the Copernicus Atmosphere Monitoring Service (CAMS). Finally, the authors thank NASA's Giovanni data system (http://giovanni.sci.gsfc.nasa.gov/giovanni/) for providing the MODIS data.

References

Alfaro, S.C., M. Abdel Wahab, 2006: Extreme variability of aerosol optical properties: the Cairo aerosol characterization experiment case study. – In: Perrin, A., et al. (Ed.): Remote Sensing of the Atmosphere for Environment Security. – Springer Verlag, The Netherlands, 285–299.

Brand, B., J. Zingerle, 2011: The renewable energy targets of the Maghreb countries: Impact on electricity supply and conventional power markets. – Energy Policy **39**, 4411–4419, DOI:10.1016/j.enpol.2010.10.010.

Bryden, J., L. Riahi, R. Zissler, 2013: MENA renewables statusreport. – Report for REN21. http://www.ren21.net/Portals/0/documents/activities/Regional%20Reports/MENA_2013_lowres.pdf (accessed on 31 March 2015).

Diabaté, L., P.H. Blanc, L. Wald, 2004: Solar radiation climate in Africa. – Solar Energy **76**, 733–744.

El-Metwally, M., 2004: Simple new methods to estimate global solar radiation based on meteorological data in Egypt. – Atmos. Res. **69**, 217–239.

El-Metwally, M., S.C. Alfaro, 2013. Correlation between meteorological conditions and aerosol characteristics at an East-Mediterranean coastal site. – Atmos. Res. **132–133**, 76–90.

El-Metwally, M., S.C. Alfaro, M.A. Wahab, B. Chatenet, 2008: Aerosol characteristics over urban Cairo: Seasonal variations as retrieved from Sun photometer measurements. – J. Geophys. Res. **113**, D14219.

El-Metwally, M., S.C. Alfaro, M.M. Abdel Wahab, A.S. Zakey, B. Chatenet, 2010: Seasonal and inter-annual variability of the aerosol content in Cairo (Egypt) as deduced from the comparison of MODIS aerosol retrievals with direct AERONET measurements. – Atmos. Res. **97**, 14–25.

El-Metwally, M., S.C. Alfaro, M.M. Abdel Wahab, O. Favez, Z. Mohamed, B. Chatenet, 2011: Aerosol properties and associated radiative effects over Cairo (Egypt). – Atmos. Res. **99**, 263–276.

El-Wakil, S.A., M. El-Metwally, C. Gueymard, 2001: Atmospheric turbidity of urban and desertic areas of the Nile basin in the aftermath of Mt. Pinatubo's eruption. – Theor. Appl. Climatol. **68**, 89–108.

El Sobki, M.S., 2015: Electricity sector in Egypt between challenges and opportunities – full scale program for renewable energy in Egypt. – Presented at the World Future Energy Summit, Abu Dhabi, UAE, 27 January 2015. http://www.mesia.com/wp-content/uploads/Sobki%20-%20NREA%20-%20AbuDhabi-January%2020-2015.pdf (accessed on 31 March 2015).

Favez, O., H. Cachier, J. Sciare, S. Alfaro, T.M. El-Araby, M.A. Harhash, M.M. Abdelwahab, 2008: Seasonality of major aerosol species and their transformations in Cairo megacity. – Atmos. Env. **42**, 1503–1516, DOI: 10.1016/j.atmosenv.2007.10.081.

Griffiths, S., 2013: Strategic considerations for deployment of solar photovoltaics in the Middle East and North Africa. – Energy. Strateg. Rev. **2**, 125–131, DOI:10.1016/j.esr.2012.11.001.

Gueymard, C.A., 1998: Turbidity determination from broadband irradiance measurements: A detailed multicoefficient approach. – J. Appl. Meteorol. Climatol. **37**, 414–435.

Gueymard, C.A., J.A. Ruiz-Arias, 2016: Extensive worldwide validation and climate sensitivity analysis of direct irradiance predictions from 1-min global irradiance. – Solar Energy. **128**, 1–30.

Gupta, P., M.N. Khan, A. da-Silva, F. Patadia, 2013: MODIS aerosol optical depth observations over urban areas in Pakistan: quantity and quality of the data for air quality monitoring. – Atmos. Poll. Res. **4**, 43–52.

Holben B.N., T.F. Eck, I. Slutsker, D. Tanré, J.P. Buis, A. Setzer, E. Vermote, J.A. Reagan, Y. Kaufman, T. Nakajima, F. Lavenu, I. Jankowiak, A. Smirnov, 1998: AERONET – A federated instrument network and data archive for aerosol characterization. – Rem. Sens. Env. **66**, 1–16.

Jalal, K.A., A. Asmat, N. Ahmad, 2015: Aerosol optical depth (AOD) retrieval method using MODIS. – In: Proceedings of the 2015 International Conference on Space Science and Communication, held on 10–12 August 2015, Langkawi, Malaysia, 370–374. [7283802] IEEE Computer Society. DOI: 10.1109/IconSpace.2015.7283802.

Korany, M., M. Boraiy, Y. Eissa, Y. Aoun, M.M. Abdel Wahab, S.C. Alfaro, P. Blanc, M. El-Metwally, H. Ghedira, K. Hungershoefer, L. Wald, 2016: A database of multi-year (2004–2010) quality-assured surface solar hourly irradiation measurements for the Egyptian territory. – Earth Syst. Sci. Data **8**, 105–113, www.earth-syst-sci-data.net/8/105/2016/, DOI:10.5194/essd-8-105-2016.

López, G., M.A. Rubio, F.J. Batlles, 2000: Estimation of hourly direct normal from measured global solar irradiance in Spain. – Renew. Energy **21**, 175–186.

Louche, A., G. Notton, P. Poggi, G. Simonnot, 1991: Correlations for direct normal and global horizontal irradiation on French Mediterranean site. – Sol. Energy **46**, 261–266.

Mahmoud, K.F., S.C. Alfaro, O. Favez, M.M. Abdel Wahab, J. Sciare, 2008: Origin of black carbon concentration peaks in Cairo (Egypt). – Atmos. Res. **89**, 161–169.

Morcrette, J.-J., O. Boucher, L. Jones, D. Salmond, P. Bechtold, A. Beljaars, A. Benedetti, A. Bonet, J.W. Kaiser, M. Razinger, M. Schulz, S. Serrar, A.J. Simmons, M. Sofiev, M. Suttie, A.M. Tompkins, A. Untch, 2009: Aerosol analysis and forecast in the European Centre for Medium-Range Weather Forecasts Integrated Forecast System: Forward modeling. – J. Geophys. Res. **114**, D06206, DOI:10.1029/2008JD011235., 2009.

Nikitidou, E., A. Kazantzidis, V. Salamalikis, 2014: The aerosol effect on direct normal irradiance in Europe under clear skies. – Renew. Energy **68**, 475–484.

Omran, M.A., 2000: Analysis of solar radiation over Egypt. – Theor. Appl. Climatol. **67**, 225–240.

Oumbe, A., Z. Qu, P. Blanc, M. Lefèvre, L. Wald, S. Cros, 2014: Decoupling the effects of clear atmosphere and clouds to simplify calculations of the broadband solar irradiance at ground level. – Geosci. Model Deveop. **7**, 1661–1669, DOI:10.5194/gmd-7-1661-2014, 2014, Corrigendum 7, 2409–2409.

WMO/CIMO, 2014: Guide to meteorological instruments and methods of observation. – World Meteorological Organization, WMO-No. **8**.

WMO-IMO, 2016: XIIth International pyrheliometer comparison (IPC XII). – Report No. **124**, Davos, Switzerland, 28 Sept.–16 October, 2015.

WRC, 1985: Sixth international pyrheliometer comparison (IPC VI). – Working Report No. **137**.

WRC, 1995: International pyrheliometer comparison (IPC VII). – Working Report No. **188**. Davos, Switzerland, 25 September–13 October.